



Cite this: *J. Mater. Chem. C*, 2022,  
10, 9723

## Realizing the efficiency-stability balance for all-polymer photovoltaic blends†

Shangfei Yao,<sup>ab</sup> Tao Yang,<sup>id</sup> <sup>\*ac</sup> Xiaodong Shen,<sup>b</sup> Tongzhou Li,<sup>b</sup> Bingzhang Huang,<sup>\*d</sup> Heng Liu,<sup>e</sup> Xinhui Lu,<sup>id</sup> <sup>e</sup> Tao Liu <sup>id</sup> <sup>\*b</sup> and Bingsuo Zou <sup>id</sup> <sup>b</sup>

Although the power conversion efficiency (PCE) of organic solar cells (OSCs) has been increased to over 19% under 1 sun illumination, stability is still a shortcoming which impedes commercialization; this has motivated researchers to pay more attention to this issue. Herein we report two types of all-polymer blends: a traditional donor-acceptor pair of PM6:PY-IT; and a one-pot synthesized, multicomponent example called PM6-*b*-PY-IT, and these exhibit different performance changes under external stress. The PM6-*b*-PY-IT device has a PCE of 13.63% which is lower than that of 15.24% for PM6:PY-IT, but it has better operational stability under continuous illumination and better thermostability, thereby realizing greater power output over a period of one month. Morphology characterization and thermal degradation process studies reveal that the PM6-*b*-PY-IT system can overcome stress, probably due to the existence of chemical bonding between the donor and acceptor phase/block, which enables stable phase separation, while excessive phase segregation in the binary all-polymer blend seriously undermines the device performance. This work provides a novel way of achieving high stability OSCs derived from a well-established all-polymer blend, which hopefully will enhance the marketing prospects for this photovoltaic technology.

Received 29th May 2022,  
Accepted 14th June 2022

DOI: 10.1039/d2tc02232j

[rsc.li/materials-c](http://rsc.li/materials-c)

## Introduction

In the past few decades, it had been hoped that organic solar cells (OSCs), would take the leading position of a new generation of photovoltaic (PV) products in the international sustainable energy market, because of their advantages including lightweight, color tunability, low toxicity, solution processability, and so on.<sup>1–12</sup> However, even though the record power conversion efficiency (PCE) has been pushed to a high level for both single-junction and tandem devices by researchers, its stability still causes the “short board effect”, reducing users’ confidence in this technology’s commercialization prospects.<sup>13–30</sup> Therefore,

the urgent issue to be solved, is the stability, or achieving the performance-stability balance for OSCs.

One promising way to gain high stability for OSCs is to develop an all-polymer photo-active system, to overcome the disadvantages of small molecular acceptors. Traditional perylene diimide (PDI) and naphthalene diimide (NDI) type polymer acceptors enabled devices give excellent stability but have inferior PCEs (<9%).<sup>31–33</sup> In recent years, the new types of polymerized small molecular acceptors endow the polymer–polymer device with a rapid increase in PCE.<sup>34–48</sup> However, this type of all-polymer blend exhibits a poorer stability due to the low molecular weight. Accordingly, material designs based on current, mature, efficient all-polymer systems aiming to promote the stability of the morphology should be a meaningful strategy. Constructing a donor-acceptor connected block copolymer is a promising method, to achieve this goal, according to recently reported progress.<sup>49–52</sup> Although the precise characterization of the component in these blends is difficult to realize, their better device stability is still a significant improvement.

In this work, we report a comparison of PCE and stability between the standout all-polymer blend PM6:PY-IT, and its counterpart PM6-*b*-PY-IT, a one-pot synthesized multicomponent system which could include: PM6, PY-IT and a co-polymer with donor and acceptor blocks chemically bonding together.<sup>52</sup> As a result, the device efficiency of a traditional binary system is 15.24%, which was consistent with values found in other

<sup>a</sup> Julong College, Shenzhen Technology University, Shenzhen 518118, China.

E-mail: [yangtao@sztu.edu.cn](mailto:yangtao@sztu.edu.cn)

<sup>b</sup> Guangxi Key Lab of Processing for Nonferrous Metals and Featured Materials and Key lab of new Processing Technology for Nonferrous Metals and Materials, Ministry of Education, School of Resources, Environments and Materials, Guangxi University, Nanning 530004, China. E-mail: [liutaozhx@gxu.edu.cn](mailto:liutaozhx@gxu.edu.cn), [zoubs@gxu.edu.cn](mailto:zoubs@gxu.edu.cn)

<sup>c</sup> Centre for Mechanical Technology and Automation, Department of Mechanical Engineering, University of Aveiro, 3810-193 Aveiro, Portugal

<sup>d</sup> School of Civil and Architectural Engineering, Liuzhou Institute of Technology, Liuzhou 545610, China. E-mail: [71889671@qq.com](mailto:71889671@qq.com)

<sup>e</sup> Department of Physics, Chinese University of Hong Kong, Hong Kong, New Territories, Hong Kong 999077, China

† Electronic supplementary information (ESI) available. See DOI: <https://doi.org/10.1039/d2tc02232j>

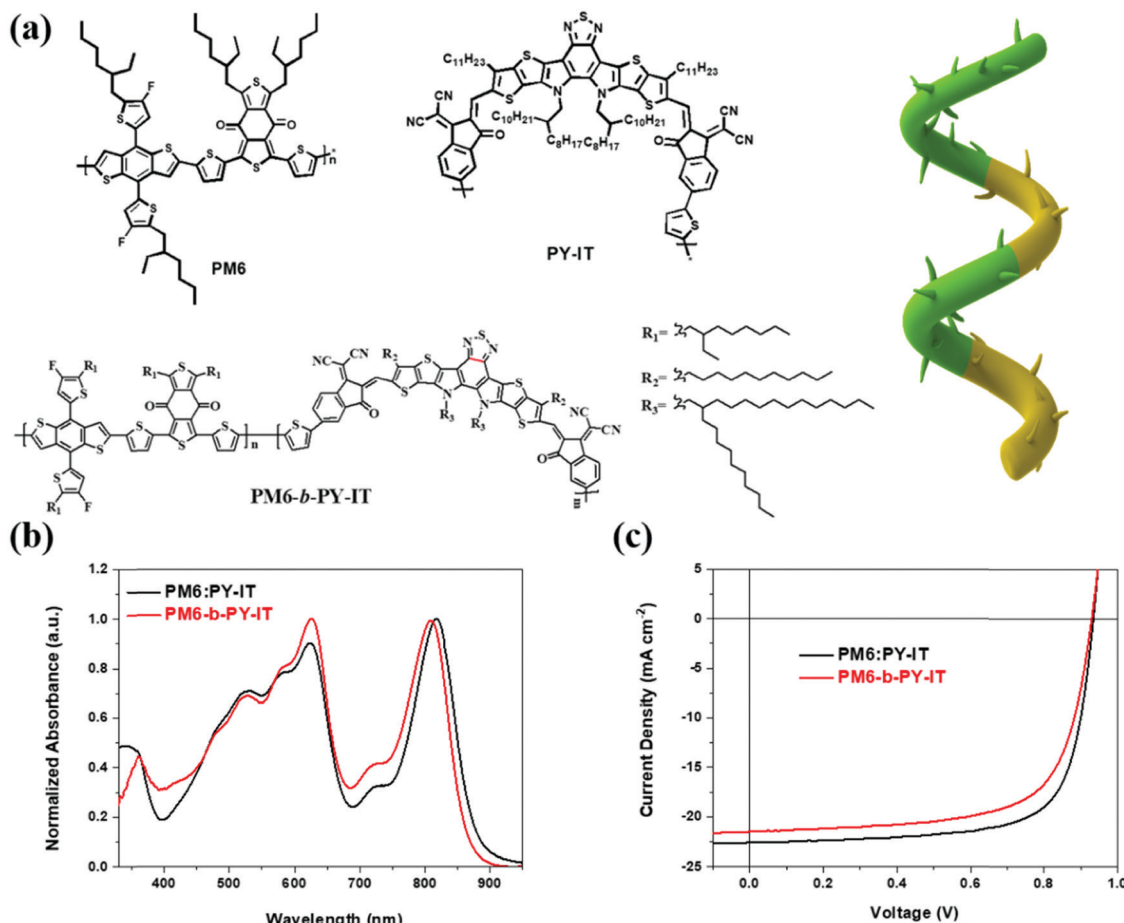


Fig. 1 (a) Chemical structures of the materials used in this work. (b) Normalized UV-vis absorbance spectra of the two systems. (c) The  $J$ - $V$  characteristics of the materials.

reports.<sup>53</sup> In contrast, the PCE of the PM6-*b*-PY-IT blend is 13.63%, but the short-circuit current density ( $J_{SC}$ ) and fill factor (FF) are lower. Although the initial PCE is lower, the PM6-*b*-PY-IT based device stability is better than that of PM6:PY-IT, both operationally and thermally. Consequently, in a one-month period, PM6-*b*-PY-IT can convert more solar energy into electricity than PM6:PY-IT can. To evaluate the morphology stability differences, we compared their thermostability and the AFM images of initial and high-temperature stressed films. It is shown that durability of thermal stress for PM6-*b*-PY-IT is much better than that of PM6:PY-IT, therefore its useful morphology features can maintain the PV performance well. The overly separated phase in the thermally degraded film of PM6:PY-IT severely undermines the long-term stability. This work presents a clear understanding of the morphology stability produced by one-pot synthesized polymer blends, and achieves an efficiency-stability balance for the OSC devices, which should be useful to the whole of the sustainable energy market field.

## Results and discussion

The PM6 and PY-IT used in this work were the same as used in previous research.<sup>52</sup> The synthetic procedures of PM6-*b*-PY-IT

are provided in the ESI.<sup>†</sup> In the measurements of high-temperature gel permeation chromatography (GPC) using 1,2-dichlorobenzene as the eluent, the number average molecular weights ( $M_n$ ) and dispersity ( $D$ ) were estimated as 23.8 kDa and 1.85, respectively. As shown in the GPC curves (Fig. S1, ESI<sup>†</sup>), PM6-*b*-PY-IT has only one peak. This result suggests two possible situations: (i) there is only a single molecular weight copolymer with PM6 and PY-IT blocks connected or (ii) there is a block copolymer, with PM6 and PY-IT co-existing in the blend, with molecular weights that are very similar. The chemical structures are presented in Fig. 1(a), and a schematic illustration for the copolymer is shown.

The thermogravimetric analysis (TGA) curves of PM6-*b*-PY-IT are shown in Fig. S2a (ESI<sup>†</sup>), and the decomposition temperature was found to be 322.7 °C. The absorption profiles of the two systems are shown in Fig. S2b (ESI<sup>†</sup>) and Fig. 1(b). Compared with the binary blend, the absorption coefficient of PM6-*b*-PY-IT was significantly lower, suggesting that it has a poorer light harvesting ability. In addition, the one-pot synthesized material enabled film has a blue shift and a rather lower acceptor peak, which suggested there was weaker acceptor aggregation, which was consistent with the principle that the block copolymer contains a donor-acceptor phase with limited separation.

Table 1 Photovoltaic parameters of the devices

Active layer	$V_{OC}$ (V)	$J_{SC}$ (mA cm $^{-2}$ )	$J_{cal}$ (mA cm $^{-2}$ )	FF (%)	PCE (%)
PM6:PY-IT	0.934 (0.934 $\pm$ 0.003)	22.60 (22.28 $\pm$ 0.31)	22.22	72.2 (72.4 $\pm$ 0.9)	15.24 (15.06 $\pm$ 0.27)
PM6- <i>b</i> -PY-IT	0.929 (0.928 $\pm$ 0.003)	21.51 (21.38 $\pm$ 0.23)	21.20	68.2 (67.9 $\pm$ 1.2)	13.63 (13.47 $\pm$ 0.24)

The average values and standard deviations were calculated from 20 independent devices.

Then we fabricated devices with the configuration ITO/PEDOT:PSS/polymer/PDINN/Ag to determine the PCE differences between the two systems. Consequently, the PCEs for PM6:PY-IT and PM6-*b*-PY-IT were 15.24% and 13.63%, respectively. The corresponding  $J$ - $V$  characteristics and parameters are given in Fig. 1(c) and Table 1. The efficiency drop was due to the decreased  $J_{SC}$  and FF. The PV performances were then checked using external quantum efficiency (EQE) as shown in the spectra in Fig. S3a (ESI $\dagger$ ), and the integrated current density values are given in Table 1. This showed that the efficiency error was strictly controlled within 2%. Notably, a 13.63% PCE was also one of the best values for one-pot synthesized polymer materials, when compared with other materials reported in the literature (Table S1, ESI $\dagger$ ).

Subsequently, the device physics of the two systems was studied. Fig. S3b (ESI $\dagger$ ) presents the charge separation and extraction properties of the devices examined in this work, which were studied by plotting the dependence of the photocurrent density ( $J_{ph}$ ) vs. effective voltage ( $V_{eff}$ ). $^{54}$  The charge generation of PM6-*b*-PY-IT and its collection probabilities were lower than that of the PM6:PY-IT blend (90.8%  $<$  91.9%; 73.5%

$<$  79.3%, respectively), which was consistent with the  $J_{SC}$  and FF comparison. Moreover, the recombination investigation was enabled by the relationship between  $V_{OC}$  vs.  $\ln(P_{light})$  and  $\lg(J_{SC})$  vs.  $\lg(P_{light})$ , where  $P_{light}$  is the light intensity. $^{55,56}$  From the plots in Fig. S3c (ESI $\dagger$ ) and Fig. 3(d), the fitted  $S$  (bimolecular recombination index) and  $n$  (ideal factor) values were 0.97 and 1.13 for PM6:PY-IT, and 0.93 and 1.20 for PM6-*b*-PY-IT, respectively. These results indicated that the PM6-*b*-PY-IT-based devices suffer higher levels of trap-assisted bimolecular recombination, which might be caused by insufficient phase separation and poor bi-continuity because of the alternately connected blocks.

In addition, the mobilities were assessed using the space charge limited current (SCLC) method. $^{57}$  The  $J$ - $V$  curves of hole-only and electron-only devices are shown in Fig. S4 (ESI $\dagger$ ). The PM6:PY-IT system achieved the hole and electron mobilities ( $\mu_h$  and  $\mu_e$ ) of  $9.02 \times 10^{-4}$  and  $5.48 \times 10^{-4}$  cm $^2$  V $^{-1}$  s $^{-1}$ , respectively, with a  $\mu_h/\mu_e$  ratio of 1.646, meanwhile the PM6-*b*-PY-IT-based system showed smaller  $\mu_h$  and  $\mu_e$  values of  $8.18 \times 10^{-4}$  and  $4.67 \times 10^{-4}$  cm $^2$  V $^{-1}$  s $^{-1}$ , respectively, with a higher  $\mu_h/\mu_e$  ratio of 1.752. The block copolymer containing film had a

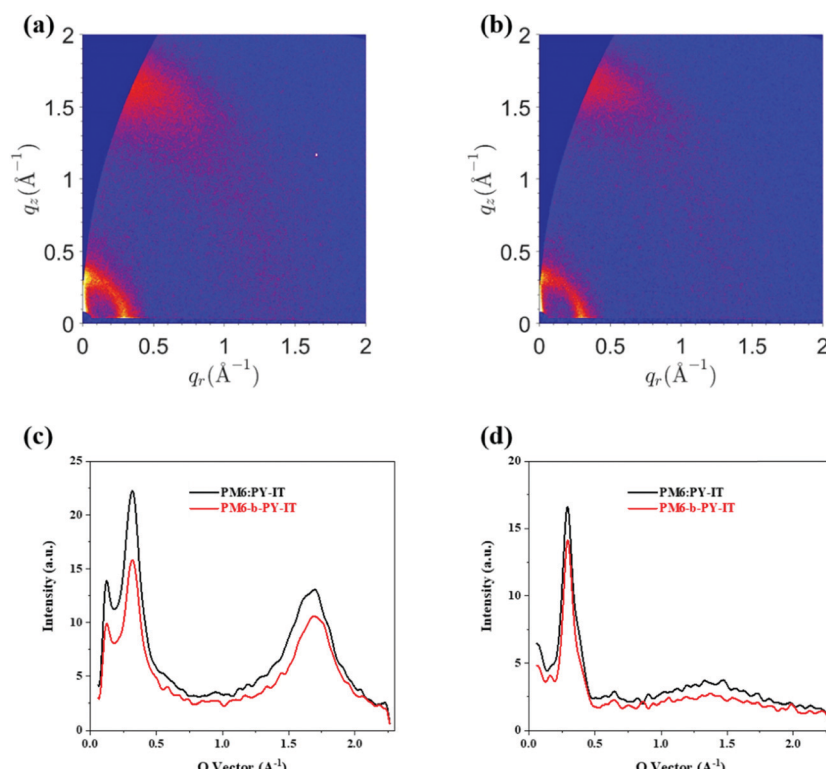


Fig. 2 The 2D-GIWAXS patterns of (a) PM6:PY-IT and (b) PM6-*b*-PY-IT. Intensity profiles based on the (c) OOP and (d) IP directional diffraction signals.

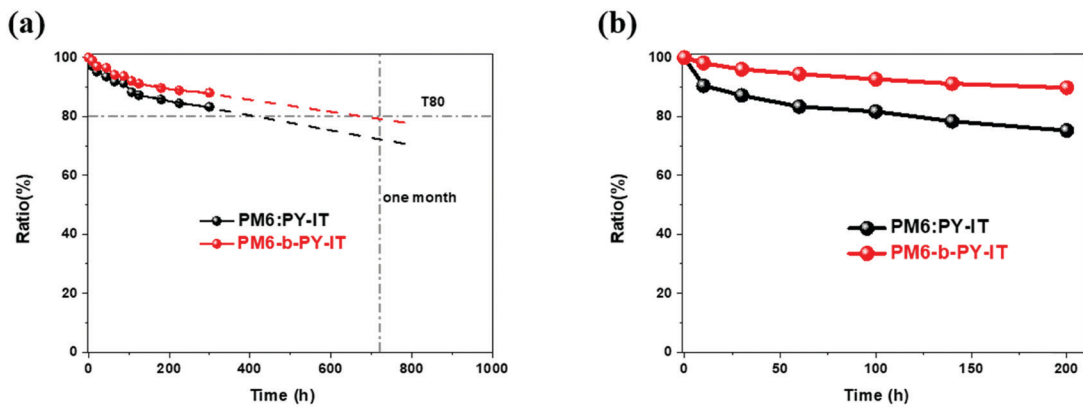


Fig. 3 (a) Operational stability, and (b) thermostability data.

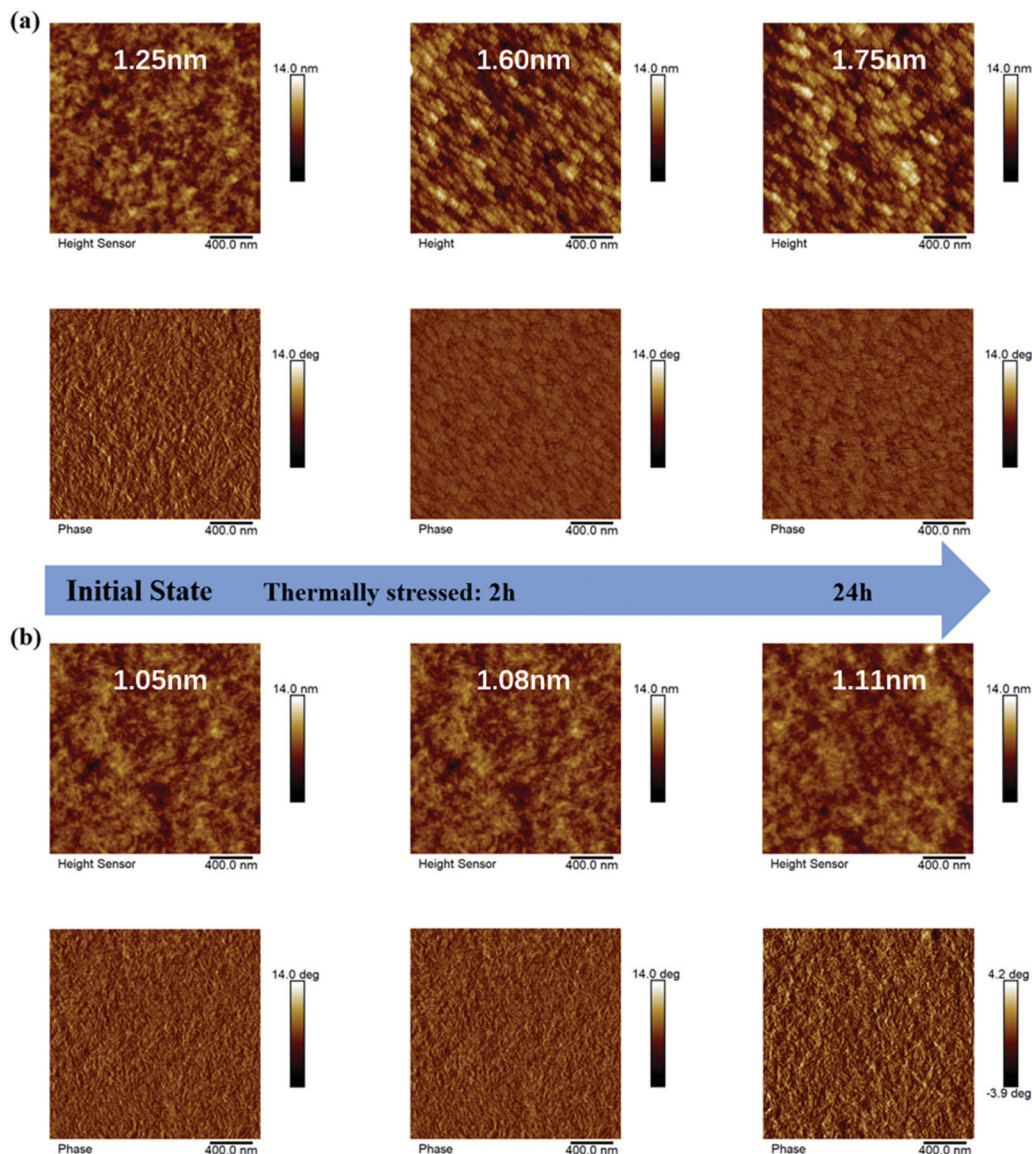


Fig. 4 AFM height (top) and phase (bottom) images of the initial state films and their thermally stressed (2 h and 24 h) states for (a) PM6:PY-IT and (b) PM6-b-PY-IT systems.

lower mobility, which might be caused by two factors: (i) the donor-acceptor alternatively connected structure, prompts limited bi-continuity and phase purity, and (ii) the molecular weight of PM6-*b*-PY-IT was not so high.

To further confirm this issue a morphology study, using grazing incidence wide-angle X-ray scattering (GIWAXS) measurement was undertaken.<sup>58–63</sup> Fig. 2(a) and (b) show 2D patterns of the binary PM6:PY-IT, and the PM6-*b*-PY-IT (one-pot produced films), whereas the fitted intensity profiles along the out-of-plane (OOP) and in-plane (IP) directions are shown in Fig. 2(c) and (d). The  $\pi$ - $\pi$  stacking peaks from the OOP direction were located at  $1.69\text{ \AA}^{-1}$  for the binary blend and  $1.70\text{ \AA}^{-1}$  for block copolymer containing one, and their lamellar diffraction peaks in the IP direction uniformly located at  $0.30\text{ \AA}^{-1}$ . The difference of the crystallinities can be observed in the quantitative comparison. The peak areas and crystalline coherence lengths (CCLs) of the  $\pi$ - $\pi$  packing showed a decreasing trend from PM6:PY-IT to PM6-*b*-PY-IT, in both directions, which was consistent with previous results relating to the device physics and the hypothesis.

After evaluating the initial PCE and the underlying mechanism, the device stability, an equally important index for device performance, was examined. As shown in Fig. 3(a), the glass encapsulated devices, under 1 sun illumination in an ambient atmosphere, of both systems were used to investigate the operational stability. The estimated T80 value of the one pot synthesized multicomponent system was significantly higher than that of its binary counterpart ( $681\text{ h} > 416\text{ h}$ ). In addition, the integrated area under the curve of PCE ratio vs time was 13% higher than that of PM6:PY-IT from 0 h to 720 h, and this indicated that PM6-*b*-PY-IT converted more solar energy (*ca.* 1%, as the initial PCE was 12% lower) in a one-month period. Practically, this is a pleasant way to determine the efficiency-stability balance, because the PVs are supposed to

be able to be used for years once they are commercialized. The first-month energy conversion amount was improved, suggesting that more energy would be continuously generated over time. In addition, we also investigated their thermostabilities, and the results in Fig. 3(b) show that after 200 h in a  $\text{N}_2$  glovebox baked at  $80\text{ }^\circ\text{C}$ , the unencapsulated devices of PM6:PY-IT retained an initial PCE of 71.3%, whereas the PCE value for PM6-*b*-PY-IT was 89.8%. These results demonstrated that the one pot synthesis method was able to produce a more stable polymer–polymer active layer, than its traditional counterparts. Furthermore, the calculations also proved that it can achieve a better efficiency-stability balance for the OSC devices.

To understand the better stability achieved, atomic force spectroscopy (AFM) tests were applied to screen the morphology evolution of the two systems from the optimized state to the thermal stress degraded ones (2 h and 24 h, at  $120\text{ }^\circ\text{C}$ ). The root-mean-square (RMS) values are marked in Fig. 4 for direct comparison. It was apparent that the thermally driven surface roughness enlargement in the PM6:PY-IT-based film outperformed that of PM6-*b*-PY-IT-based one, which might be evidence of a stronger phase separation induced by such strong external stress. According to the phase images, PM6:PY-IT exhibited a morphological feature near the thermodynamic equilibrium after high temperature processing, whereas the PM6-*b*-PY-IT film maintained its initial general phase separation. These phenomena indicated that the existence of chemically bonded donor-acceptor blocks can resist external stress induced over phase segregation.

To demonstrate this change, a schematic diagram is also provided (Fig. 5). Semi-*para*-crystalline PM6 and PY-IT undergo continuous phase separation and coarsening when the films are subjected to an external driving force. This characteristic makes the device exhibit a lower  $J_{\text{SC}}$  due to less donor/acceptor interface, reduced  $V_{\text{OC}}$  because of more serious recombination



Fig. 5 Schematic diagrams of the morphology evolution of the two systems under external stress.

loss, and poorer FF caused by inferior first-order recombination. However, the chemical bond donor and acceptor blocks could maintain their own crystallization and distribution in the film. Although there might be independent PM6 and PY-IT phases which would be affected by external stress, the block copolymer will reduce such a tendency. Therefore, its morphology stability might be better than that of the traditional donor/acceptor binary system.

## Conclusions

In summary, the one-pot synthesis of a multicomponent system, PM6-*b*-PY-IT, which achieves better efficiency-stability balance than its mainstream all-polymer blend counterpart, PM6:PY-IT, is reported. Further characterization studies show that although it has a poorer initial PCE, because it has less crystallinity and rational phase separation, its morphological stability benefits from these disadvantages. This work gives new insight into developing more stable OSCs with acceptable PCEs.

## Author contributions

Shangfei Yao: investigation, methodology, formal analysis, writing – original draft; Tao Yang: investigation, funding acquisition, resources, supervision, writing – original draft, writing – review and editing; Xiaodong Shen: investigation; Tongzhou Li: investigation; Bingzhang Huang: investigation, resources, supervision; Heng Liu: investigation; Xinhui Lu: resources; Tao Liu: conceptualization, resources, supervision, project administration; Bingsuo Zou: resources, supervision.

## Conflicts of interest

There are no conflicts to declare.

## Acknowledgements

We appreciate instruction from Prof. Alex-K-Y. Jen and Dr Qunping Fan relating to the one-pot polymerization experiments. T. Yang appreciates funding from the projects: PTDC/EME-REN/1497/2021, UIDB/00481/2020 and UIDP/00481/2020 – Fundação para a Ciência e a Tecnologia and CENTRO-01-0145-FEDER-022083 – Centro Portugal Regional Operational Programme (Centro2020), under the PORTUGAL 2020 Partnership Agreement, through the European Regional Development Fund, Shenzhen Key Laboratory of Marine Energies and Environmental Safety (ZDSYS20201215154000001) and Shenzhen Overseas Talent Project (No. GDRC202102).

## References

- 1 G. Li, V. Shrotriya, J. Huang, Y. Yao, T. Moriarty, K. Emery and Y. Yang, *Nat. Mater.*, 2005, **4**, 864–868.
- 2 Y. Li, *Acc. Chem. Res.*, 2012, **45**, 723–733.
- 3 J. Hou, O. Inganäs, R. H. Friend and F. Gao, *Nat. Mater.*, 2018, **17**, 119–128.
- 4 Y.-W. Su, S.-C. Lan and K.-H. Wei, *Mater. Today*, 2012, **15**, 554–562.
- 5 A. Facchetti, *Mater. Today*, 2013, **16**, 123–132.
- 6 P. Cheng, G. Li, X. W. Zhan and Y. Yang, *Nat. Photonics*, 2018, **12**, 131–142.
- 7 D. Deng, Y. Zhang, J. Zhang, Z. Wang, L. Zhu, J. Fang, B. Xia, Z. Wang, K. Lu, W. Ma and Z. Wei, *Nat. Commun.*, 2016, **7**, 13740.
- 8 W. Xu and F. Gao, *Mater. Horiz.*, 2018, **5**, 206–221.
- 9 X. Xu, Y. Li and Q. Peng, *Nano Sel.*, 2020, **1**, 30–58.
- 10 X. Li, I. Angunawela, Y. Chang, J. Zhou, H. Huang, L. Zhong, A. Liebman-Pelaez, C. Zhu, L. Meng, Z. Xie, H. Ade, H. Yan and Y. Li, *Energy Environ. Sci.*, 2020, **13**, 5028–5038.
- 11 G. Wang, J. Zhang, C. Yang, Y. Wang, Y. Xing, M. A. Adil, Y. Yang, L. Tian, M. Su, W. Shang, K. Lu, Z. Shuai and Z. Wei, *Adv. Mater.*, 2020, **32**, 2005153.
- 12 Y. Jiang, X. Dong, L. Sun, T. Liu, F. Qin, C. Xie, P. Jiang, L. Hu, X. Lu, X. Zhou, W. Meng, N. Li, C. J. Brabec and Y. Zhou, *Nat. Energy*, 2022, **7**, 352–359.
- 13 C. He, Z. Chen, T. Wang, Z. Shen, Y. Li, J. Zhou, J. Yu, H. Fang, Y. Li, S. Li, X. Lu, W. Ma, F. Gao, Z. Xie, V. Coropceanu, H. Zhu, J.-L. Bredas, L. Zuo and H. Chen, *Nat. Commun.*, 2022, **13**, 2598.
- 14 R. Ma, C. Yan, P. W. K. Fong, J. Yu, H. Liu, J. Yin, J. Huang, X. Lu, H. Yan and G. Li, *Energy Environ. Sci.*, 2022, **15**, 2479–2488.
- 15 R. Ma, T. Yang, Y. Xiao, T. Liu, G. Zhang, Z. Luo, G. Li, X. Lu, H. Yan and B. Tang, *Energy Environ. Mater.*, 2021, DOI: [10.1002/eem.21226](https://doi.org/10.1002/eem.21226).
- 16 Y. Cui, Y. Xu, H. Yao, P. Bi, L. Hong, J. Zhang, Y. Zu, T. Zhang, J. Qin, J. Ren, Z. Chen, C. He, X. Hao, Z. Wei and J. Hou, *Adv. Mater.*, 2021, **33**, 2102420.
- 17 Z. Zheng, J. Wang, P. Bi, J. Ren, Y. Wang, Y. Yang, X. Liu, S. Zhang and J. Hou, *Joule*, 2022, **6**, 171–184.
- 18 K. Chong, X. Xu, H. Meng, J. Xue, L. Yu, W. Ma and Q. Peng, *Adv. Mater.*, 2022, **34**, 2109516.
- 19 H. Meng, C. Liao, M. Deng, X. Xu, L. Yu and Q. Peng, *Angew. Chem., Int. Ed.*, 2021, **60**, 22554–22561.
- 20 L. Zhan, S. Li, Y. Li, R. Sun, J. Min, Z. Bi, W. Ma, Z. Chen, G. Zhou, H. Zhu, M. Shi, L. Zuo and H. Chen, *Joule*, 2022, **6**, 662–675.
- 21 S. Chen, L. Feng, T. Jia, J. Jing, Z. Hu, K. Zhang and F. Huang, *Sci. China: Chem.*, 2021, **64**, 1192–1199.
- 22 L. Zhu, M. Zhang, J. Xu, C. Li, J. Yan, G. Zhou, W. Zhong, T. Hao, J. Song, X. Xue, Z. Zhou, R. Zeng, H. Zhu, C.-C. Chen, R. C. I. MacKenzie, Y. Zou, J. Nelson, Y. Zhang, Y. Sun and F. Liu, *Nat. Mater.*, 2022, **21**, 656–663.
- 23 X. Duan, W. Song, J. Qiao, X. Li, Y. Cai, H. Wu, J. Zhang, X. Hao, Z. Tang, Z. Ge, F. Huang and Y. Sun, *Energy Environ. Sci.*, 2022, **15**, 1563–1572.
- 24 Z. Luo, R. Ma, J. Yu, H. Liu, T. Liu, F. Ni, J. Hu, Y. Zou, A. Zeng, C.-J. Su, U. S. Jeng, X. Lu, F. Gao, C. Yang and H. Yan, *Natl. Sci. Rev.*, 2022, nwac076, DOI: [10.1093/nsr/nwac076](https://doi.org/10.1093/nsr/nwac076).

25 C. Yan, J. Yu, Y. Li, P. W. K. Fong, R. Ding, K. Liu, H. Xia, Z. Ren, X. Lu, J. Hao and G. Li, *Matter*, 2022, DOI: [10.1016/j.matt.2022.04.028](https://doi.org/10.1016/j.matt.2022.04.028).

26 J. Yu, X. Liu, Z. Zhong, C. Yan, H. Liu, P. W. K. Fong, Q. Liang, X. Lu and G. Li, *Nano Energy*, 2022, **94**, 106923.

27 R. Ma, Y. Tao, Y. Chen, T. Liu, Z. Luo, Y. Guo, Y. Xiao, J. Fang, G. Zhang, X. Li, X. Guo, Y. Yi, M. Zhang, X. Lu, Y. Li and H. Yan, *Sci. China: Chem.*, 2021, **64**, 581–589.

28 Y. Li, X. Huang, K. Ding, H. K. M. Sheriff, L. Ye, H. Liu, C.-Z. Li, H. Ade and S. R. Forrest, *Nat. Commun.*, 2021, **12**, 5419.

29 X. Du, T. Heumueller, W. Gruber, A. Classen, T. Unruh, N. Li and C. J. Brabec, *Joule*, 2019, **3**, 215–226.

30 Y. Qin, N. Balar, Z. Peng, A. Gadisa, I. Angunawela, A. Bagui, S. Kashani, J. Hou and H. Ade, *Joule*, 2021, **5**, 2129–2147.

31 K. Feng, J. Huang, X. Zhang, Z. Wu, S. Shi, L. Thomsen, Y. Tian, H. Y. Woo, C. R. McNeill and X. Guo, *Adv. Mater.*, 2020, **32**, 2001476.

32 Y. Zhou, T. Kurosawa, W. Ma, Y. Guo, L. Fang, K. Vandewal, Y. Diao, C. Wang, Q. Yan, J. Reinspach, J. Mei, A. L. Appleton, G. I. Koleilat, Y. Gao, S. C. B. Mannsfeld, A. Salleo, H. Ade, D. Zhao and Z. Bao, *Adv. Mater.*, 2014, **26**, 3767–3772.

33 N. Zhou and A. Facchetti, *Mater. Today*, 2018, **21**, 377–390.

34 H. Sun, B. Liu, Y. Ma, J.-W. Lee, J. Yang, J. Wang, Y. Li, B. Li, K. Feng, Y. Shi, B. Zhang, D. Han, H. Meng, L. Niu, B. J. Kim, Q. Zheng and X. Guo, *Adv. Mater.*, 2021, **33**, 2102635.

35 T. Jia, J. Zhang, K. Zhang, H. Tang, S. Dong, C.-H. Tan, X. Wang and F. Huang, *J. Mater. Chem. A*, 2021, **9**, 8975–8983.

36 R. Ma, J. Yu, T. Liu, G. Zhang, Y. Xiao, Z. Luo, G. Chai, Y. Chen, Q. Fan, W. Su, G. Li, E. Wang, X. Lu, F. Gao, B. Tang and H. Yan, *Aggregate*, 2021, e58.

37 T. Liu, T. Yang, R. Ma, L. Zhan, Z. Luo, G. Zhang, Y. Li, K. Gao, Y. Xiao, J. Yu, X. Zou, H. Sun, M. Zhang, T. A. Dela Peña, Z. Xing, H. Liu, X. Li, G. Li, J. Huang, C. Duan, K. S. Wong, X. Lu, X. Guo, F. Gao, H. Chen, F. Huang, Y. Li, Y. Li, Y. Cao, B. Tang and H. Yan, *Joule*, 2021, **5**, 914–930.

38 Q. Fan, H. Fu, Z. Luo, J. Oh, B. Fan, F. Lin, C. Yang and A. K. Y. Jen, *Nano Energy*, 2022, **92**, 106718.

39 W. Zhang, C. Sun, I. Angunawela, L. Meng, S. Qin, L. Zhou, S. Li, H. Zhuo, G. Yang, Z.-G. Zhang, H. Ade and Y. Li, *Adv. Mater.*, 2022, **34**, 2108749.

40 R. Ma, K. Zhou, Y. Sun, T. Liu, Y. Kan, Y. Xiao, T. A. Dela Peña, Y. Li, X. Zou, Z. Xing, Z. Luo, K. S. Wong, X. Lu, L. Ye, H. Yan and K. Gao, *Matter*, 2022, **5**, 725–734.

41 J. Du, K. Hu, J. Zhang, L. Meng, J. Yue, I. Angunawela, H. Yan, S. Qin, X. Kong, Z. Zhang, B. Guan, H. Ade and Y. Li, *Nat. Commun.*, 2021, **12**, 5264.

42 Y. Zhang, B. Wu, Y. He, W. Deng, J. Li, J. Li, N. Qiao, Y. Xing, X. Yuan, N. Li, C. J. Brabec, H. Wu, G. Lu, C. Duan, F. Huang and Y. Cao, *Nano Energy*, 2022, **93**, 106858.

43 S. Ding, R. Ma, T. Yang, G. Zhang, J. Yin, Z. Luo, K. Chen, Z. Miao, T. Liu, H. Yan and D. Xue, *ACS Appl. Mater. Interfaces*, 2021, **13**, 51078–51085.

44 Z. Genene, J.-W. Lee, S.-W. Lee, Q. Chen, Z. Tan, B. A. Abdulahi, D. Yu, T.-S. Kim, B. J. Kim and E. Wang, *Adv. Mater.*, 2022, **34**, 2107361.

45 C. Sun, J.-W. Lee, S. Seo, S. Lee, C. Wang, H. Li, Z. Tan, S.-K. Kwon, B. J. Kim and Y.-H. Kim, *Adv. Energy Mater.*, 2022, **12**, 2103239.

46 C. Liao, Y. Gong, X. Xu, L. Yu, R. Li and Q. Peng, *Chem. Eng. J.*, 2022, **435**, 134862.

47 T. Wang, R. Sun, W. Wang, H. Li, Y. Wu and J. Min, *Chem. Mater.*, 2021, **33**, 761–773.

48 Y. Li, J. Song, Y. Dong, H. Jin, J. Xin, S. Wang, Y. Cai, L. Jiang, W. Ma, Z. Tang and Y. Sun, *Adv. Mater.*, 2022, **34**, 2110155.

49 S. Li, X. Yuan, Q. Zhang, B. Li, Y. Li, J. Sun, Y. Feng, X. Zhang, Z. Wu, H. Wei, M. Wang, Y. Hu, Y. Zhang, H. Y. Woo, J. Yuan and W. Ma, *Adv. Mater.*, 2021, **33**, 2101295.

50 Y.-W. Su, Y.-C. Lin and K.-H. Wei, *J. Mater. Chem. A*, 2017, **5**, 24051–24075.

51 S. H. Park, Y. Kim, N. Y. Kwon, Y. W. Lee, H. Y. Woo, W.-S. Chae, S. Park, M. J. Cho and D. H. Choi, *Adv. Sci.*, 2020, **7**, 1902470.

52 Z. Luo, T. Liu, R. Ma, Y. Xiao, L. Zhan, G. Zhang, H. Sun, F. Ni, G. Chai, J. Wang, C. Zhong, Y. Zou, X. Guo, X. Lu, H. Chen, H. Yan and C. Yang, *Adv. Mater.*, 2020, **32**, 2005942.

53 R. Ma, M. Zeng, Y. Li, T. Liu, Z. Luo, Y. Xu, P. Li, N. Zheng, J. Li, Y. Li, R. Chen, J. Hou, F. Huang and H. Yan, *Adv. Energy Mater.*, 2021, **11**, 2100492.

54 Y. Wu, Y. Zheng, H. Yang, C. Sun, Y. Dong, C. Cui, H. Yan and Y. Li, *Sci. China: Chem.*, 2020, **63**, 265–271.

55 R. Ma, Y. Chen, T. Liu, Y. Xiao, Z. Luo, M. Zhang, S. Luo, X. Lu, G. Zhang, Y. Li, H. Yan and K. Chen, *J. Mater. Chem. C*, 2020, **8**, 909–915.

56 H. Zhao, B. Lin, J. Xue, H. B. Naveed, C. Zhao, X. Zhou, K. Zhou, H. Wu, Y. Cai, D. Yun, Z. Tang and W. Ma, *Adv. Mater.*, 2022, **34**, 2105114.

57 T. Yang, R. Ma, H. Cheng, Y. Xiao, Z. Luo, Y. Chen, S. Luo, T. Liu, X. Lu and H. Yan, *J. Mater. Chem. A*, 2020, **8**, 17706–17712.

58 X. Jiang, P. Chotard, K. Luo, F. Eckmann, S. Tu, M. A. Reus, S. Yin, J. Reitenbach, C. L. Weindl, M. Schwartzkopf, S. V. Roth and P. Müller-Buschbaum, *Adv. Energy Mater.*, 2022, **12**, 2103977.

59 J. Rivnay, S. C. B. Mannsfeld, C. E. Miller, A. Salleo and M. F. Toney, *Chem. Rev.*, 2012, **112**, 5488–5519.

60 R. Ma, T. Liu, Z. Luo, K. Gao, K. Chen, G. Zhang, W. Gao, Y. Xiao, T.-K. Lau, Q. Fan, Y. Chen, L.-K. Ma, H. Sun, G. Cai, T. Yang, X. Lu, E. Wang, C. Yang, A. K. Y. Jen and H. Yan, *ACS Energy Lett.*, 2020, **5**, 2711–2720.

61 Y.-C. Lin, H.-W. Cheng, Y.-W. Su, B.-H. Lin, Y.-J. Lu, C.-H. Chen, H.-C. Chen, Y. Yang and K.-H. Wei, *Nano Energy*, 2018, **43**, 138–148.

62 Y.-C. Lin, C.-H. Chen, N.-Z. She, C.-Y. Juan, B. Chang, M.-H. Li, H.-C. Wang, H.-W. Cheng, A. Yabushita, Y. Yang and K.-H. Wei, *J. Mater. Chem. A*, 2021, **9**, 20510–20517.

63 Y.-C. Lin, Y.-J. Lu, C.-S. Tsao, A. Saeki, J.-X. Li, C.-H. Chen, H.-C. Wang, H.-C. Chen, D. Meng, K.-H. Wu, Y. Yang and K.-H. Wei, *J. Mater. Chem. A*, 2019, **7**, 3072–3082.